



STRUCTURAL BIOLOGY
COMMUNICATIONS

Volume 75 (2019)

Supporting information for article:

**Structural characterization of a prolyl aminodipeptidase (PepX)
from *Lactobacillus helveticus***

Deanna Dahlke Ojennus, Nicholas J. Bratt, Kent L. Jones and Douglas H. Juers

Table S1 Ramachandran plot analysis of the catalytic acid, catalytic histidine, and the neighboring residue of the catalytic histidine in representative structures of the Group A catalytic acid zone (Dimitriou *et al.*, 2017, 2019) as well as PepX enzymes.

	<i>PDB</i>	<i>Catalytic Acid</i>	<i>Catalytic Histidine</i> ⁱ	<i>Histidine Neighbor</i> ⁱ	<i>Ramachandran Plot</i> ^j
Carboxylesterase	3WJ2_A ^a	D251	H281 (56)	I280 (19)	Favored
Carboxylesterase	1LZL_A ^b	D260	H290 (3)	F289 (12)	Favored
Cholesterol esterase	1LLF_A ^c	E341	H449 (34)	F448 (18)	Favored
Hydroxynitrilase	3C6X_A ^d	D207	H235 (34)	D234 (18)	Allowed
Acylamino-acid-releasing enzyme	2HU5_A ^e	D524	H556 (80)	G555 (11)	Allowed
Salicylic acid-binding protein 2	1XKL_A ^f	D210	H238 (64)	D237 (2)	Allowed
Acetylxylian esterase	1G66_A ^g	D175	H187 (73)	T186 (67)	Favored
PepX <i>L. lactis</i>	1LNS_A ^h	D468	H498 (0.8)	A497 (0.3)	Outlier
PepX <i>L. helveticus</i>	6NFF_A	D483	H514 (5)	P513 (0.01)	Outlier

^a(Ohara *et al.*, 2014)

^b(Zhu *et al.*, 2003)

^c(Pletnev *et al.*, 2003)

^d(Schmidt *et al.*, 2008)

^e(Kiss *et al.*, 2007)

^f(Forouhar *et al.*, 2005)

^g(Ghosh *et al.*, 2001)

^h(Rigolet *et al.*, 2002)

ⁱNumber in parentheses is the energy percentile ranking by MobProbit (Chen *et al.*, 2010). A lower number indicates higher energy relative to the other residues. Note that in all cases except for 1LZL, the residue neighboring the catalytic histidine exhibits higher backbone strain energy than the histidine.

^jCatalytic histidine neighbor assigned as either favored, allowed, or outlier based on DeepView (Guex & Peitsch, 1997) Ramachandran plot analysis.

Table S2 Comparison of conserved binding/active site residues between the *L. helveticus* PepX (6NFF) with *L. lactis* PepX (1LNS) and DPP-IV (1R9N) (Rigolet *et al.*, 2005).

The single amino acid difference between *L. helveticus* and *L. lactis* is shown in bold.

	<i>L. helveticus</i>	<i>L. lactis</i>	Human	Location
	PepX	PepX	DPP-IV	
Catalytic Triad				
Serine	S363	S348	S630	Catalytic Domain
Aspartate	D483	D468	D708	Catalytic Domain
Histidine	H514	H498	H740	Catalytic Domain
Positioning of Substrate				
Residue 1	Y395	Y380	Y662	Helical Domain
Residue 2	L416	L401	Y666	Helical Domain
Residue 3	W392	W377	W659	Helical Domain
Residue 4	I389	I374	V656	Helical Domain
Specificity Pocket				
Residue 1	N485	N470	N710	Catalytic Domain
Residue 2	V486	V471	V711	Catalytic Domain
Oxyanion Hole				
Residue 1	Y364	Y349	Y631	Catalytic Domain
Residue 2	Y229	Y210	Y547	Catalytic Domain
Exopeptidase Activity				
Residue 1	C408	F393	E205	Helical Domain
Residue 2	E411	E396	E206	Helical Domain

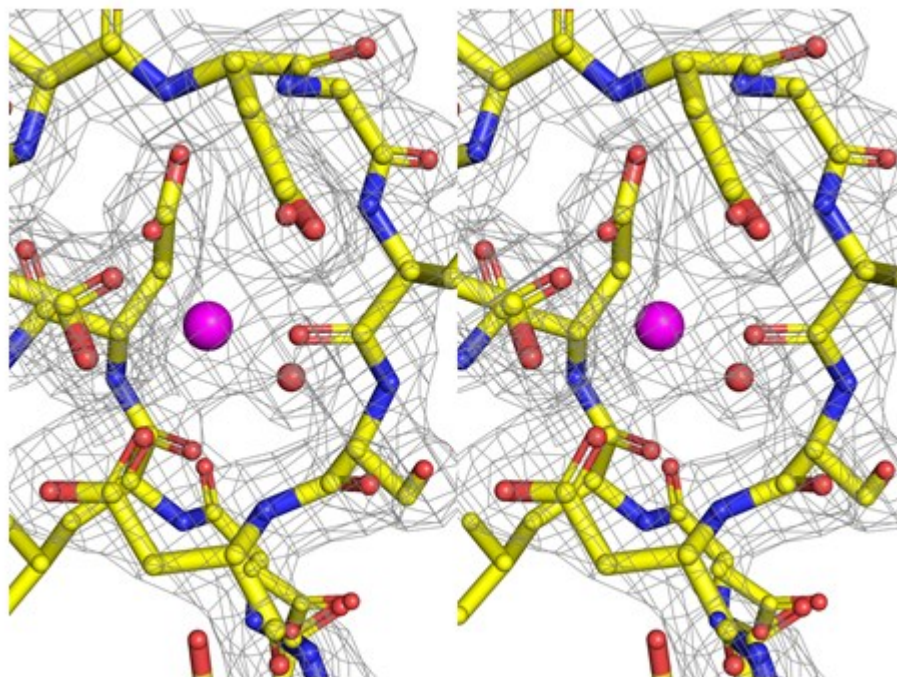


Figure S1 Wall-eyed stereo view prepared in Pymol (Schrödinger, LLC.) of 2Fo-Fc electron density with final refined coordinates at the calcium binding site. Atom colors are C: yellow, O: red, N:blue, Ca: magenta. The density is contoured at 1.5 r.m.s.d. The view is roughly the same as in Figure 1c.

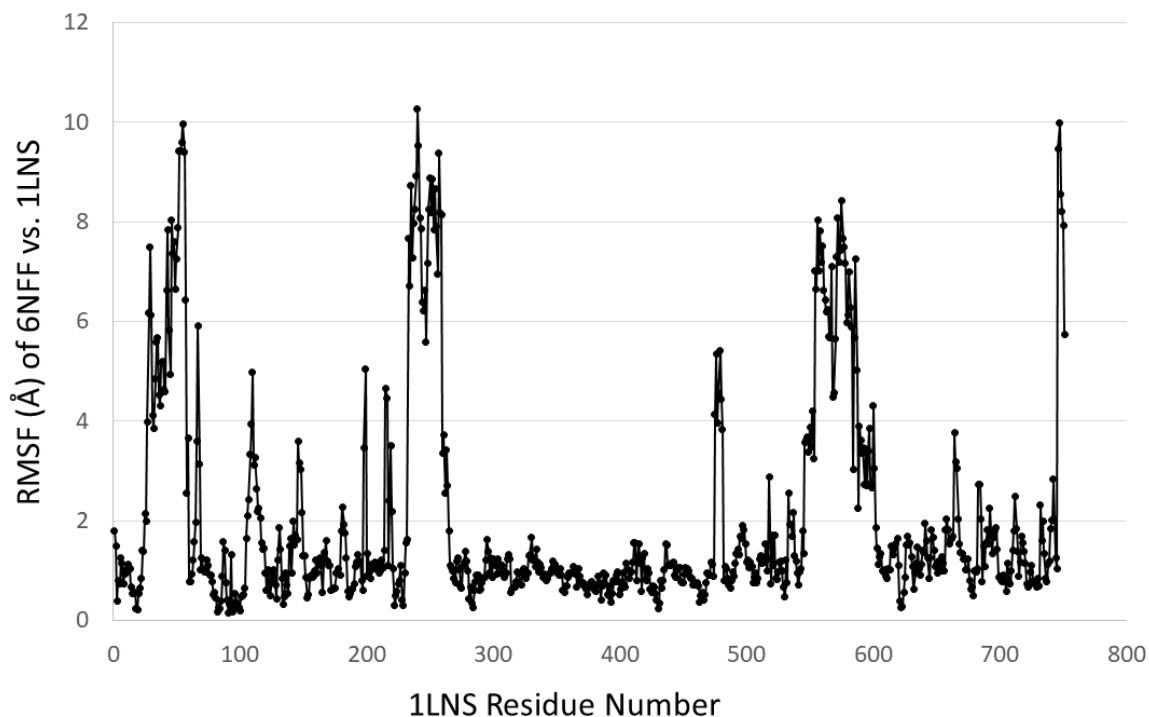


Figure S2 Root mean square fluctuation in superposition of 6NFF onto 1LNS with gaps in alignment removed as calculated by Bio3d (Grant *et al.*, 2006). Residue numbering is for 1LNS. Three major regions of divergence, where more than ten sequential residues diverge by more than 2 Å, are observed. Residues 25-58 correspond to the second and third helix of 1LNS. In 6NFF an extra three residue 3_{10} helix is observed between helix 1 and 2 and helix 4 (3 in 1LNS) is longer. Residues 234-262 correspond to the “lasso loop”. Residues 549-601 are located in the first two strands and helices of the C-terminal domain. In 6NFF, an extra three residue 3_{10} helix is located prior to the first strand, the first strand is shorter and an extra three residue strand immediately follows the first strand in an anti-parallel configuration which is not observed in 1LNS. Also, helix 1 of 1LNS in the C-terminal domain lies nearly orthogonal to the helix observed in 6NFF.

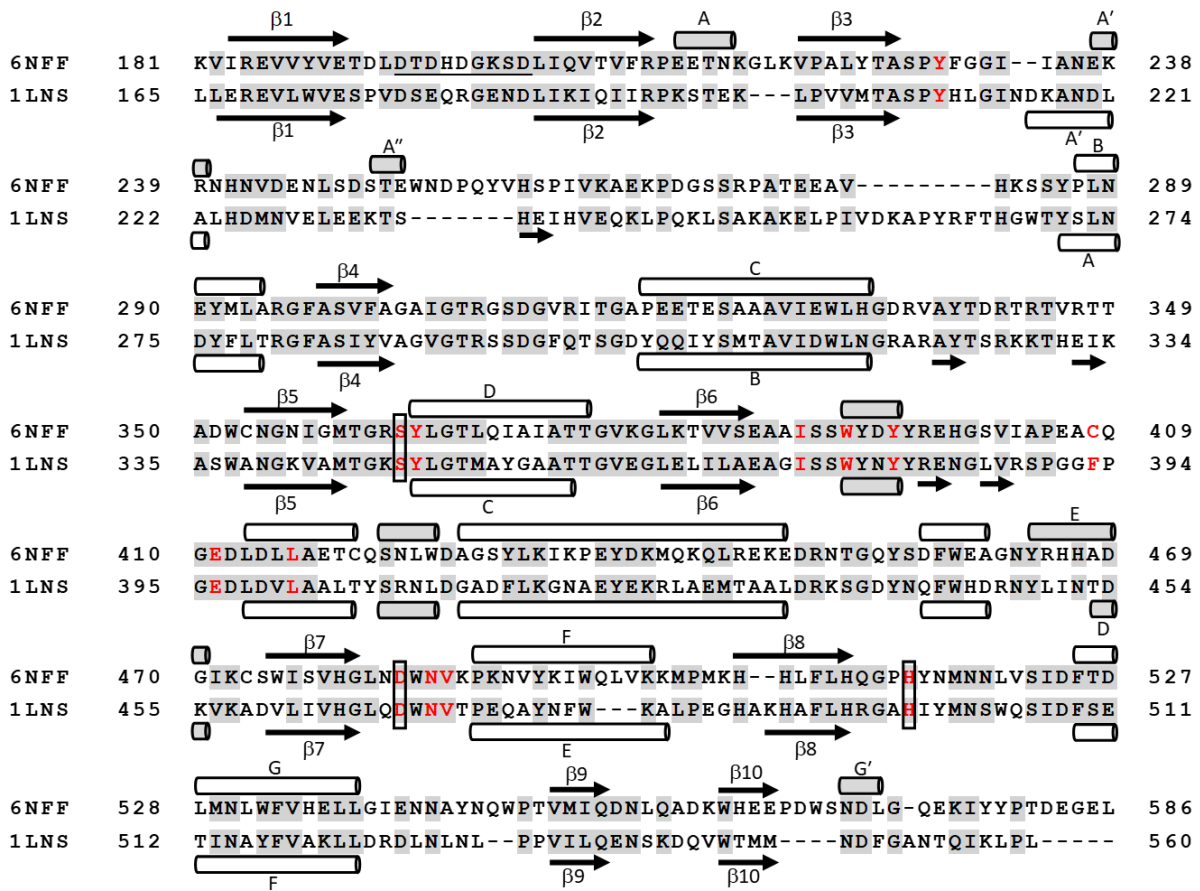


Figure S3 Sequence alignment created with protein BLAST (Altschul *et al.*, 1997, 2005) of the 6NFF and 1LNS catalytic and helical domains. Conserved residues are highlighted in gray. The catalytic triad residues are boxed. Residues postulated to interact with substrate at the binding site are shown in red. The calcium blade zone sequence which gives rise to the calcium-binding blade-like site of 6NFF is underlined. Secondary structures are defined by STRIDE (Heinig & Frishman, 2004) and indicated with arrows and cylinders. Cylinders representing 3₁₀ helices are shaded gray.